Electron-Stimulated Chemical Reactions in Carbon Tetrachloride/Water (Ice) Films

A. J. Wagner, C. Vecitis, and D. H. Fairbrother*

Department of Chemistry, The Johns Hopkins University, 3400 N. Charles Street, Baltimore, Maryland 21218

Received: October 3, 2001; In Final Form: February 10, 2002

The electron-stimulated chemical reactions in carbon tetrachloride/water (ice) and ice films have been studied using reflection−absorption infrared spectroscopy (RAIRS) and mass spectrometry. CO_2, CO, and HCl were identified as the final neutral reaction products in the electron-stimulated degradation of CCl_4, while $COCl_2$ and C_2Cl_4 were produced as intermediates. Molecular H_2 and O_2 were detected as neutral gas-phase products in the electron beam irradiation of pure ice films. Production of molecular oxygen was, however, efficiently quenched during irradiation of CCl_4/H_2O(ice) mixtures. A reaction mechanism is postulated based on the reactivity of the trichloromethyl ($^{\bullet}CCl_3$) radical and dichlorocarbene ($:CCl_2$) intermediates. Reactions between the trichloromethyl ($^{\bullet}CCl_3$) radical and oxygen or hydroxyl radicals lead to the production of phosgene, the subsequent electron-stimulated decomposition of which produces CO or CO_2. In contrast, reactions involving dichlorocarbene produce CO via hydrolysis or C_2Cl_4 as a result of a carbon−carbon coupling reaction.

Introduction

Chlorinated solvents are widely used in industry with applications as lubricants and cleaning solvents and in the chemical processing of nuclear materials.[1] Exposure to chlorinated hydrocarbons even for very low exposures is, however, believed to result in a number of adverse health effects.[2] Consequently, there has been increasing concern in the past decade over the environmental and health impact of chlorocarbons.[3] Under ambient conditions, however, many chlorocarbons do not degrade readily.[4,5] As a result, a number of methods have been developed for the degradation of chlorinated hydrocarbons over the past decade, and their mechanisms have been studied. These include incineration,[6] photocatalysis,[7] sonolysis,[8] electrochemical dehalogenation,[9] microbial systems,[10] catalytic decomposition over metal oxides,[11] and reactions with metallic iron[12] and mineral surfaces.[13]

The reactivity of electrons with water and chlorinated compounds has also lead to the emergence of electron beam technology as an effective remediation strategy.[14] For example, researchers have shown that electron beam irradiation can destroy chloroform, trichloromethane, trichloroethylene, and tetrachloroethylene[15] in contaminated groundwater. The interaction of high-energy (>100 eV) electrons with water produces a cascade of low energy (<10 eV) solvated secondary electrons ($e^-_{(aq)}$) as well as a number of very reactive intermediates, most notably $^{\bullet}OH$ and $^{\bullet}H$ radicals.[16] These reactive species go on to react with chlorine containing organics leading to their destruction.[16] For example, the initial reactions associated with carbon tetrachloride removal by electron irradiation in solution are:[17]

$$CCl_4 + e^-_{(aq)} \rightarrow {}^{\bullet}CCl_3 + Cl^- \quad (k = 1.3 \times 10^{10}\ M^{-1}\ s^{-1}) \quad (1)$$

$$CCl_4 + H^{\bullet} \rightarrow {}^{\bullet}CCl_3 + HCl \quad (k = 3.2 \times 10^{7}\ M^{-1}\ s^{-1}) \quad (2)$$

On the basis of these relative rate constants, the initial step in the destruction of carbon tetrachloride is believed to involve dissociative electron attachment.

The chemical identity of reactive intermediates formed during electron-mediated degradation of CCl_4 in aqueous environments has been probed directly by Choi and Hoffman[18] in a study of CCl_4 photoreduction in the presence of TiO_2. With the use of 2,3-dimethyl-2-butene to trap transient free radical intermediates, the initial electron-transfer step was shown to involve both one- and two-electron-transfer reactions leading to the production of trichloromethyl radical and dichlorocarbene species, thus;

$$CCl_4 + e^-_{(aq)} \rightarrow {}^{\bullet}CCl_3 + Cl^-_{(aq)} \quad (e^-_{(aq)} = \text{solvated electron}) \quad (1)$$

$$^{\bullet}CCl_3 + e^-_{(aq)} \rightarrow :CCl_2 + Cl^-_{(aq)} \quad (3)$$

In oxygenated aqueous solutions, the trichloromethyl radical reacts rapidly with dissolved oxygen:[19]

$$^{\bullet}CCl_3 + O_2 \rightarrow CCl_3OO^{\bullet} \quad (4)$$

Decomposition of the peroxyl radical generates a phosgene intermediate, the subsequent hydrolysis of which under ambient conditions produces CO_2 and HCl. In contrast, dichlorocarbene can form tetrachloroethylene,[20,21]

$$:CCl_2 + :CCl_2 \rightarrow C_2Cl_4 \quad (5)$$

or react with water to form carbon monoxide and hydrochoric acid,[22]

$$:CCl_2 + H_2O \rightarrow 2HCl + CO \quad (6)$$

Through the use of infrared spectroscopy, the nature of carbon containing species produced during the low-energy (30−200 eV) electron bombardment of an Ar/CCl_4 matrix at 12 K has also been studied by Suzer and Andrews.[23] Direct spectroscopic evidence of the trichloromethyl radical ($^{\bullet}CCl_3$), dichlorocarbene

* To whom correspondence should be addressed.

10.1021/jp013697z CCC: $22.00
Published on Web 03/30/2002

(:CCl_2), and tetrachloroethylene (C_2Cl_4) was found although hexachloroethane (C_2Cl_6) was not observed.

For chlorofluorocarbons (CFCs) coadsorbed on top of ice films, the importance of solvated electrons has also been noted by Lu and Madey who reported enhancements factors of 10^2-10^4 in electron-induced dissociation experiments.[24-26] This phenomena has been attributed to the efficient trapping of low-energy secondary electrons by water or ammonia clusters generating solvated electrons. Electron transfer to C−Cl-containing species produces a vibrationally excited intermediate that dissociates to produce halide anions. These results also have potentially significant implications in the stratosphere where the very low free electron density has typically been used to argue that electron-induced processes are unimportant for CFC destruction.

The identification and energy distribution of species produced during the interaction of <200 eV electrons with amorphous D_2O ice (D-ice) films have been investigated by Orlando and co-workers.[27-32] Various neutral gas-phase products have been identified including atomic D and O, as well as D_2 and O_2. In related studies, Prince et al.[33] reported that excited •OH radicals were detected during the interaction of 15−50 eV electrons with ice, while in a related study Noell et al. reported the production of H^+ above 21 eV.[34] Electron-stimulated desorption of D^- has also been reported by Rowntree et al. for incident electron energies in the 5−15 eV range.[35]

In this study, we report on the dominant chemical transformations and associated neutral reaction products that accompany electron irradiation of CCl_4/H_2O(ice) films. The systems serve as models for electron-stimulated dechlorination reactions in deoxygenated aqueous solutions. During electron beam irradiation, carbon dioxide, carbon monoxide, molecular hydrogen, and hydrochloric acid were identified as gas-phase reaction products, while carbon dioxide, phosgene, and tetrachloroethylene were observed in the ice film. The production of gas-phase molecular oxygen, detected in the electron beam irradiation of pure ice films, was quenched during irradiation of CCl_4/H_2O(ice) films. A reaction mechanism is postulated based on the reactivity of both the trichloromethyl (•CCl_3) radical and dichlorocarbene (:CCl_2) intermediates produced as the result of initial dissociative electron attachment to CCl_4.

Experimental Section

Experiments were carried out in an ultrahigh vacuum (UHV) chamber equipped with a Physical Electronics 04-500 Dual Anode X-ray source, Physical Electronics 10-360 single channel analyzer, Balzers Prisma quadrupole mass spectrometer for gas analysis, and a custom designed chamber for reflection−absorption infrared measurements.[36] The X-ray photoelectron spectra (XPS) chamber was pumped directly by a 200 L s^{-1} ion pump, and the infrared chamber was pumped by a 230 L s^{-1} turbomolecular pump. In the absence of a system bake-out, this pumping arrangement allowed a base pressure of 1×10^{-8} Torr to be maintained.

CCl_4/H_2O(ice) films were condensed onto a polycrystalline Au (99.99%, Accumet) mirror mounted on a copper sample holder attached to a ceramic feedthrough coupled to an UHV sample manipulator. The sample was cooled by passing liquid nitrogen into a stainless steel tube connected to the feed-through. This arrangement enabled temperatures of ∼100 K to be maintained during experiments, as measured by a chromel−alumel thermocouple attached directly to the front face of the substrate. Sample heating was achieved by replacing the flow of liquid nitrogen with gaseous nitrogen.

Reflectance−absorption infrared (RAIR) measurements were carried out using a Mattson Infinity series FTIR spectrometer equipped with external beam capabilities. Experiments carried out in this investigation employed a narrow-band mercury−cadmium−telluride (MCT) detector (700−4000 cm^{-1}). RAIR spectra were recorded using a resolution of 4 cm^{-1} by summing 500 scans. All scans were referenced to the Au surface at ∼100 K before CCl_4/H_2O dosing. X-ray photoelectron spectra (XPS) were recorded using Mg Kα X-ray radiation (1253.6 eV) at 15 kV and 300 W with a 45° takeoff angle with respect to the sample normal.

Carbon tetrachloride ($^{12}CCl_4$ Aldrich (99.9%); $^{13}CCl_4$ Cambridge Isotopes (99%)) and water (Millipore, deionized) were stored in separate glass vacuum bulbs attached to a gas manifold. CCl_4 and H_2O were both subject to several freeze−pump−thaw cycles before use. The vapor for each compound was then expanded into an isolated volume prior to mixing in the gas manifold. The CCl_4/H_2O mixture was typically allowed to stabilize for ∼10 min prior to dosing onto the cooled Au substrate through a UHV leak valve. During dosing, gas purity was checked using mass spectrometry.

Electrons were generated from either the unshielded output of the X-ray source operating at 300 W or a low-energy flood gun (Specs 15/40) using 4 mA emission current and a 10 eV extraction voltage. In typical experiments, a sample bias of +200 V was employed to accelerate the kinetic energy of the incident electrons and increase the rate of chemical transformation in the CCl_4/H_2O(ice) films. Although the rates of chemical reactions were sensitive to the characteristics of the electron source and the magnitude of the applied bias voltage, the same chemical transformations were observed for CCl_4/H_2O(ice) films using the X-ray source or the electron gun in the absence or presence of an applied bias voltage.

Results

Initial CCl_4/H_2O(Ice) Film Characterization. Figure 1a shows the XPS spectra of a CCl_4/H_2O(ice) film deposited on the Au mirror at ∼100 K. In the XPS spectra of the CCl_4/H_2O-(ice) film (Figure 1a), the largest peaks at 535.2, 271.8, and 202.0 eV can be assigned to the O(1s), Cl(2s), and Cl(2p) transitions, respectively, while the smaller feature at 291.0 eV can be identified as the C(1s) transition of *C*Cl_4. No peak was observed at 83.8 or 87.5 eV due to the Au($4f_{7/2}$ /$4f_{5/2}$) transition associated with the substrate, respectively. This indicates that the CCl_4/H_2O(ice) film is at least 300 Å thick.[36] On the basis of the integrated XP areas of the Cl(2p) and O(1s) transitions and their respective XPS sensitivity factors,[37] the typical CCl_4/H_2O(ice) films used to obtain the results shown in Figures 2−5 have a CCl_4/H_2O ratio of ∼1:2.7.

Figure 1b shows a typical RAIR spectrum of a $^{13}CCl_4/H_2O$-(ice) film deposited at ∼100 K. The spectrum is dominated by a broad feature between 3000 and 3600 cm^{-1} associated with the O−H stretching mode of adsorbed H_2O and the Fermi doublet of $^{13}CCl_4$ composed of the ν_3 stretching mode observed at 780 cm^{-1} and the $\nu_1 + \nu_4$ combination mode at 758 cm^{-1}.[38,39] The weaker ν_2 bending mode of water can also be resolved as a broad feature between 1600 and 1700 cm^{-1}. These assignments, as well as those corresponding to $^{12}CCl_4$, are shown in Table 1. A negative absorbance feature is also visible in Figure 1 at 939 cm^{-1}. Separate experiments on the evolution of the RAIR spectra as a function of $^{13}CCl_4/H_2O$ exposure time revealed that the integrated IR area of this negative absorbance feature at 939 cm^{-1} was directly proportional to the integrated area of the $^{13}CCl_4$ peaks. As a result, we have assigned this

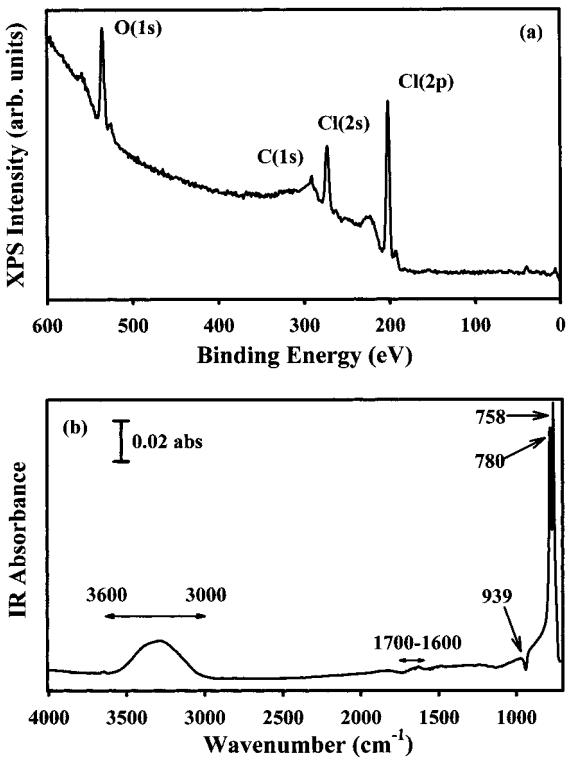

Figure 1. Characterization of representative CCl_4/H_2O(ice) films employed in this study following deposition on the Au substrate at ~100 K before electron beam irradiation. Panel a shows the X-ray photoelectron spectroscopy results. The positions of the primary O(1s), C(1s), Cl(2s), and Cl(2p) XP transitions are shown. On the basis of the integrated XP area of the Cl(2p) and O(1s) transitions and their respective XPS sensitivity factors, the CCl_4/H_2O ratio is calculated to be ~1:2.7. Panel b shows the RAIR spectra of a $^{13}CCl_4/H_2O$(ice) film. The O−H stretching mode of adsorbed H_2O can be observed between 3000 and 3600 cm^{-1}, as well as the weaker bending mode between 1600 and 1700 cm^{-1}. The $^{13}CCl_4$ Fermi doublet is visible at 780 and 758 cm^{-1}. The negative absorbance feature visible at 939 cm^{-1} has been ascribed to an optical interference effect caused by the $^{13}CCl_4/H_2O$(ice) film thickness. See text for details.

TABLE 1: Vibrational Assignment of Infrared Peaks Observed in the Present Investigation (All Values in cm^{-1})

observed frequency	assignment	mode description
3000−3600	H_2O	υ(O−H)
2339	$^{12}CO_2$	$\upsilon(^{12}C{=}O)$
2272	$^{13}CO_2$	$\upsilon(^{13}C{=}O)$
1798	$^{12}COCl_2$	$\upsilon(^{12}C{=}O)$
1758	$^{13}COCl_2$	$\upsilon(^{13}C{=}O)$
1560−1950	H_3O^+	$\delta_a(H_3O^+)$
1600−1700	H_2O	$\delta(H_2O)$
1180−1250	H_3O^+	$\delta_s(H_3O^+)$
914	$^{12}C_2Cl_4$	$\upsilon(^{12}C{-}Cl_2)$
885	$^{13}C_2Cl_4$	$\upsilon(^{13}C{-}Cl_2)$
855	$^{13}COCl_2$	$\upsilon(^{12}C{-}Cl_2)$
825	$^{13}COCl_2$	$\upsilon(^{13}C{-}Cl_2)$
798	$^{12}CCl_4$	$\upsilon(^{12}C{-}Cl)$
780	$^{13}CCl_4$	$\upsilon(^{13}C{-}Cl)$
767	$^{12}CCl_4$	$(\upsilon_1 + \upsilon_4)$
758	$^{13}CCl_4$	$(\upsilon_1 + \upsilon_4)$

feature to an optical interference effect caused by the $^{13}CCl_4/H_2O$(ice) film thickness.

Effect of Electron Beam Irradiation. During electron beam (e-beam) irradiation, complimentary information was obtained by combining RAIR spectra on the nature of chemical species produced in the film with mass spectrometry measurements on the chemical identity of stable neutral gas-phase species produced during electron beam irradiation.

RAIRS Results. The changes in the RAIR spectra of a typical $^{13}CCl_4/H_2O$(ice) film as a function of e-beam exposure at ~100 K are shown in Figure 2a−e. It should be noted that the $^{13}CCl_4$ Fermi doublet has been removed from Figure 2b−e for clarity. Several new peaks centered at 2339, 2272, 1758, 885, and 825 cm^{-1} can be observed in Figure 2b−e. A broader new IR band is also produced between 1560 and 1950 cm^{-1} and another weaker feature between 1180 and 1250 cm^{-1} (Figure 2). The appearance of these new IR bands is accompanied by a decrease in the $^{13}CCl_4$ Fermi doublet intensity and a significant broadening and red shift in the O−H stretching band. For comparison, Figure 2f shows the corresponding RAIR spectrum of a $^{12}CCl_4/H_2O$(ice) film exposed to e-beam irradiation for 60 min. Figure 2f shows new RAIRS peaks at 1798, 914, and 855 cm^{-1}. Figure 2f also exhibits RAIRS peaks at 2339 cm^{-1} and the broader feature between 1560 and 1950 cm^{-1} observed in Figure 2e. It should also be noted that in separate experiments on films with similar CCl_4/H_2O ratios, the RAIR signal intensities of new bands associated with product species (e.g., 1758 cm^{-1}) scaled with the thickness of the ice film (measured by the integrated area of the υ(O−H) mode). This result indicates that the reactions reported in the present investigation occur within the CCl_4/H_2O(ice) film rather than at the surface of the Au mirror.

Figure 3 shows an expanded view of the region between 950 and 700 cm^{-1} for $^{12}CCl_4/H_2O$(ice) (spectrum a) and $^{13}CCl_4/H_2O$(ice) (spectrum b) films following 60 min of electron beam irradiation. The CCl_4 Fermi doublet can be seen to increase in frequency from 780 and 758 cm^{-1} in the $^{13}CCl_4/H_2O$(ice) film to 798 and 767 cm^{-1}, respectively, in the $^{12}CCl_4/H_2O$(ice) film.[40] Electron-induced RAIRS peaks are visible at 885 and 825 cm^{-1} for the $^{13}CCl_4/H_2O$(ice) film, blue-shifting to 914 and 855 cm^{-1}, respectively, when $^{12}CCl_4/H_2O$(ice) films were employed.

Product Identification from RAIR Spectra. The new infrared absorption bands observed during electron irradiation (Figures 2 and 3) can be assigned to a combination of the following species: $COCl_2$, CO_2, C_2Cl_4, and H_3O^+(see Table 1). The $\upsilon(^{12}C{=}O)$ mode of phosgene is red-shifted in the CCl_4/H_2O(ice) film (1798 cm^{-1}) compared to its gas-phase value (1827 cm^{-1}),[41] presumably because of intermolecular interactions with water and or other phosgene molecules. The υ(C=O) mode of phosgene has previously been observed to red shift when adsorbed on a hydroxylated TiO_2 surface[42] indicating the sensitivity of this mode to intermolecular bonding. Support for the production of phosgene rather than other possible intermediates, notably formyl chloride ($\upsilon(^{12}C{=}O)$ = 1784 cm^{-1}(gas), $\upsilon(^{12}C{-}Cl)$ = 734 cm^{-1}(gas)), during electron beam irradiation of CCl_4/H_2O(ice) films is also provided by the fact that the intensity ratio of the IR modes at 1758 cm^{-1} ($\upsilon(^{13}C{=}O)$) and 825 cm^{-1} ($\upsilon(^{13}C{-}Cl_2)$) remains constant during electron irradiation (see Figure 2), indicating that they are associated with a common species.

The new broad absorption features observed are all similar to modes observed by Devlin and co-workers[43] in an infrared study of HCl in ice surfaces and are consistent with the formation of the (hydrated) hydronium ion (H_3O^+): 1560−1950 cm^{-1} (antisymmetric bend) and between 1180 and 1250 cm^{-1} (symmetric bend) as well as a weaker feature centered at ~2100 cm^{-1} (combination mode) (see Table 1). The broadening and red shifting of the υ(O−H) stretching mode is also consistent with previous studies on the effect of H_3O^+ production in ice films.[43,44] Similarly, the ratio of the OH stretching mode to the symmetric bend is seen to decrease significantly in the presence of H_3O^+ (Figure 2a−d), consistent with results reported by Barone et al.[45]

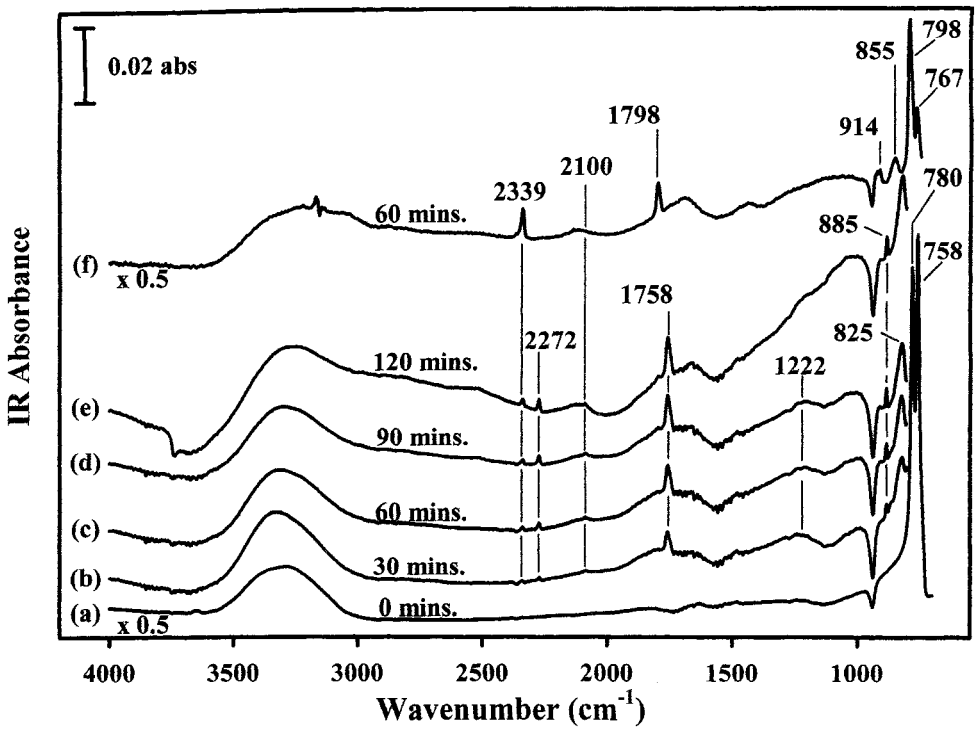

Figure 2. Variation in RAIR spectra between 700 and 4000 cm^{-1} of a $^{13}CCl_4/H_2O$(ice) film as a function of electron irradiation time. It should be noted that the $^{13}CCl_4$ Fermi doublet has been removed from spectra b−e for clarity. Line f shows the corresponding RAIR spectrum of a $^{12}CCl_4/H_2O$(ice) film after 60 min of electron irradiation.

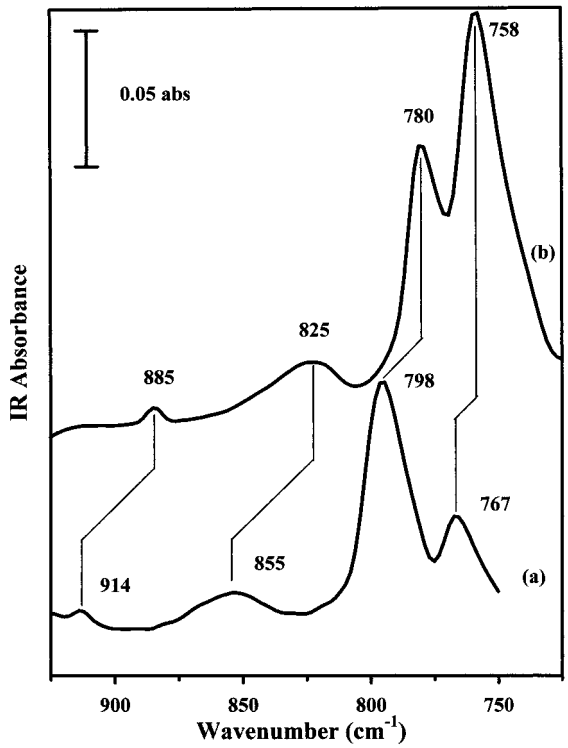

Figure 3. AIR spectra between 700 and 950 cm^{-1} for (a) $^{12}CCl_4/H_2O$(ice) and (b) $^{13}CCl_4/H_2O$(ice) films following 60 min of electron beam exposure.

Figure 4 shows the variation in the integrated IR areas for the carbon-containing species ($COCl_2$, CO_2, C_2Cl_4, and CCl_4) as a function of electron beam exposure. The CCl_4 content of the film decayed continuously during irradiation, while the $COCl_2$, CO_2, and C_2Cl_4 species initially increased in intensity before decreasing at longer irradiation times.

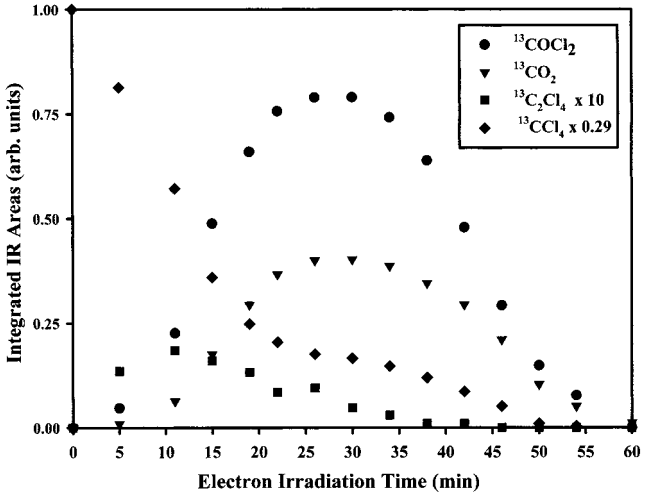

Figure 4. Integrated absorbance of infrared bands for the carbon-containing species, $^{13}COCl_2$ (●), $^{13}CO_2$ (▼), $^{13}C_2Cl_4$ (■), $^{13}CCl_4$ (♦), observed during the electron beam irradiation of $^{13}CCl_4/H_2O$(ice) films as a function of irradiation time.

Mass Spectrometry Results. The mass spectra (0−70 amu) of neutral products observed under different experimental conditions are shown in Figure 5. Figure 5a shows the mass spectrum of a $^{12}CCl_4/H_2O$ mixture during the initial gas-phase exposure onto the Au substrate held at ~100 K. Figure 5a shows that the mass spectrum is consistent with the presence of molecular $^{12}CCl_4$ with peaks at $m/q = 12$ (C^+), 35 ($^{35}Cl^+$), 37 ($^{37}Cl^+$), 47 ($C^{35}Cl^+$), and 49 ($C^{37}Cl^+$). Additional peaks with $m/q > 70$ were also observed during CCl_4 dosing, consistent with the presence of molecular CCl_4. In contrast, molecular H_2O gave rise to peaks at $m/q = 18$ (H_2O^+), 17 (OH^+), 16 (O^+), and 1 (H^+).

Figure 5b shows the mass spectrum of volatile species produced during the electron beam irradiation of a pure water

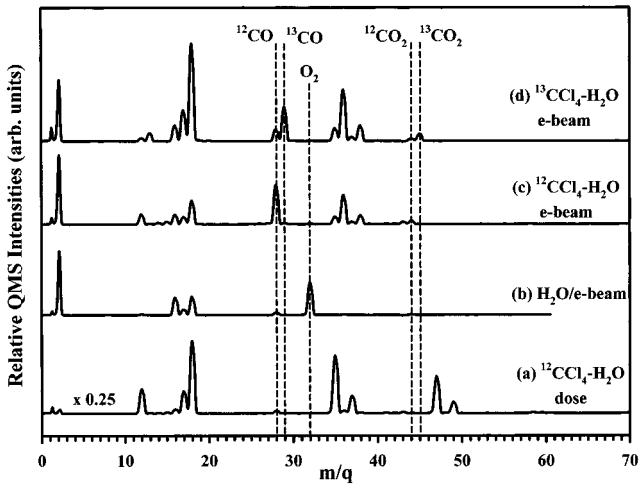

Figure 5. The mass spectra (0−70 amu) of neutral volatile species during (a) the initial gas-phase exposure of a $^{12}CCl_4/H_2O$ mixture onto the Au substrate held at ∼100 K, (b) electron beam irradiation of a pure water(ice) film, (c) electron beam irradiation of a $^{12}CCl_4/H_2O$-(ice) mixture, and (d) electron beam irradiation of a $^{13}CCl_4/H_2O$(ice) mixture. It should be noted that although only $m/q = 0-70$ are shown in Figure 5, spectra were recorded up to $m/q = 200$. Except for the case of line a for which spectral intensity associated with parent CCl_4 molecules (e.g., CCl_2^+) was observed, no spectral intensity above $m/q = 70$ was detected for lines b−d. It should be noted that ^{12}CO and $^{12}CO_2$ are detected in line d as residual gas-phase species.

film. In addition to the observation of H_2O, as well as the electron-stimulated production of H_2 ($m/q = 2$), Figure 5b illustrates that molecular oxygen ($m/q = 32$, $m/q = 16$) is also produced. The evolution of H_2 and O_2 is consistent with results from previous investigations on the nature of species produced during electron beam irradiation of water (ice) films.[30,31] Figure 5c shows the mass spectrum of volatile species produced during the electron beam irradiation of a $^{12}CCl_4/H_2O$(ice) mixture. Compared to Figure 5a, there is no evidence of any peaks associated with molecular $^{12}CCl_4$ (i.e., absence of $m/q = 47$ and 49 due to $^{12}C^{35}Cl^+$ and $^{12}C^{37}Cl^+$) and only a small amount of H_2O is observed to be desorbing. New peaks were, however, observed at $m/q = 28$ and 44, indicative of the production of CO and CO_2 during electron beam irradiation. Similarly, the fragmentation pattern observed between $m/q = 35-38$ is consistent with the production of $H^{35/37}Cl$. The production of CO and CO_2 during electron beam irradiation was also confirmed by the appearance of new peaks at $m/q = 29$ (^{13}CO) and 45 ($^{13}CO_2$) during electron beam irradiation experiments using $^{13}CCl_4/H_2O$(ice) (Figure 5d). Figure 5c and d shows that during electron-beam irradiation of $^{12/13}CCl_4/H_2O$(ice) mixtures, no evidence of molecular oxygen was observed even though the yield of molecular hydrogen is similar (compare Figure 5 spectrum b with spectra c and d).

Discussion

Reactivity of CCl_4/H_2O(ice) Films in the Absence of Electron Beam Irradiation. The stability of CCl_4/H_2O(ice) films in the absence of electron beam irradiation was examined by monitoring the RAIR spectra of a CCl_4/H_2O(ice) film held at ∼100 K over a 2−3 h time period. No chemical transformations were observed except for adsorption of background $^{12}CO_2$ evidenced by the appearance of IR intensity at 2339 cm^{-1} (for example, see Figure 2). The unwanted effect of $^{12}CO_2$ adsorption on product identification and reaction kinetics was avoided by using $^{13}CCl_4$. RAIRS experiments also revealed that warming CCl_4/H_2O(ice) films adsorbed at 100 K resulted in the loss of CCl_4 and H_2O IR peaks and the production of no new chemical species, consistent with the molecular adsorption/desorption characteristics of CCl_4 in H_2O.[46] Consequently, any changes observed in the present investigation can be ascribed to the effect of electron beam irradiation.

SCHEME 1: Dominant Reaction Steps Responsible for the Neutral Products Observed during Electron Beam Irradiation of CCl_4/H_2O(Ice) Films

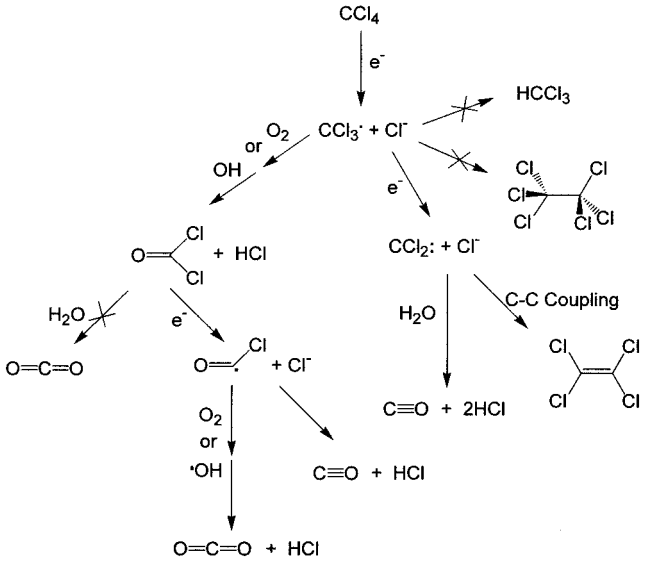

Proposed Reaction Mechanism for Electron-Mediated CCl_4 Remediation in Ice Films. On the basis of results from previous studies,[15,16,18,20,23,33] the interaction of electrons with CCl_4/H_2O(ice) films is expected to generate a range of reactive species, most notably $^\bullet CCl_3$, $:CCl_2$, H, and OH. Consequently, the products observed in this study are a result of chemical interactions between these species, as well as parent H_2O and CCl_4 molecules. The proposed principal chemical reactions responsible for the formation of the carbon-containing species observed in this study are shown in Scheme 1. In summary, the chemical reactions of CCl_4 are postulated to involve reactions of the $^\bullet CCl_3$ (trichloromethyl radical) and $:CCl_2$ (dichlorocarbene) intermediates produced as a result of the sequential one- or two-electron transfer that characterizes the initial dissociative electron capture step:[18]

$$CCl_4 + e^-_{(aq)} \rightarrow {}^\bullet CCl_3 + Cl^- \quad (1)$$

$$^\bullet CCl_3 + e^-_{(aq)} \rightarrow :CCl_2 + Cl^- \quad (3)$$

The nature of the carbon-containing products observed during electron beam irradiation can be ascribed to the reactions associated with the $^\bullet CCl_3$ and $:CCl_2$ intermediates. Evidence for the production of $:CCl_2$ is provided by the observation of $Cl_2C{=}CCl_2$,[10,47,48] while evidence of the formation of $^\bullet CCl_3$ as a transient intermediate in the CCl_4/H_2O(ice) film is based on previous studies that have correlated phosgene production with reactions of the trichloromethyl radical.[19,49,50]

Dichlorocarbene ($:CCl_2$) Intermediate. The clearest evidence for the production of $:CCl_2$ during electron beam irradiation of CCl_4/H_2O(ice) is provided by the appearance of new IR bands associated with the antisymmetric $C-Cl_2$ stretch of $^{12}C_2Cl_4$, observed at 914 cm^{-1} (Figures 2 and 3).[51] This assignment is also strongly supported by the isotopic shift calculated for $^{13}C_2Cl_4$ (observed 885 cm^{-1}, calculated[52] 884 cm^{-1}). Tetrachloroethylene formation is postulated to result from

carbon−carbon coupling of the $:CCl_2$ intermediate:

$$:CCl_2 + :CCl_2 \rightarrow Cl_2C{=}CCl_2 \quad (5)$$

The observation and importance of $:CCl_2$ coupling has been noted by previous researchers during reactions of CCl_4 with sodium carbonate[47] and various oxide surfaces[53] and in studies involving the photoreductive[20] and sonochemical[8] degradation of CCl_4. Figure 4 indicates that the concentration of C_2Cl_4 increases rapidly at short irradiation times before decaying under the influence of prolonged electron beam irradiation. This time-dependent behavior is consistent with the concentration of C_2Cl_4 in the film determined by a bimolecular production step (eq 5) and electron beam degradation ($Cl_2C{=}CCl_2 + e^- \rightarrow$ products). Preliminary experiments indicate that electron-beam-stimulated degradation of C_2Cl_4 in ice produces CO and CO_2.[54]

Hydrolysis of $:CCl_2$. In addition to carbon−carbon coupling, dichlorocarbene also reacts rapidly with water, liberating carbon monoxide and hydrochloric acid:[22]

$$H_2O + :CCl_2 \rightarrow (HO)CHCl_2 \rightarrow HOCCl + HCl \rightarrow CO + HCl \quad (7)$$

$$\textbf{Net:} \quad :CCl_2 + H_2O \rightarrow 2HCl + CO \quad (6)$$

The mechanism involves the initial insertion of $:CCl_2$ into the O−H bond of water, leading to the formation of $(HO)CHCl_2$.[55] Subsequent sequential elimination of 2 mol of HCl leads to CO formation. Under the experimental conditions (film temperature $\approx$ 100 K), any CO produced is expected to desorb ($\Delta H_{vap}(CO) = 6$ kJ mol^{-1}).[56] This assertion is consistent with the mass spectrum results shown in Figure 5, indicating that $^{12/13}CO$ is evolved during the electron beam irradiation of $^{12/13}CCl_4/H_2O$-(ice), while there is no evidence of CO in the CCl_4/H_2O(ice) film's RAIR spectrum shown in Figure 2.

Reaction 6 also leads to HCl production. Previous studies have shown that HCl undergoes ionization in ice films at ~100 K to give H_3O^+ and Cl^-:[43]

$$H_2O + HCl \rightarrow H_3O^+ + Cl^- \quad (8)$$

The production of HCl during electron beam irradiation of CCl_4/H_2O(ice) films is consistent with the appearance of new broad IR bands between 1560 and 1950 cm^{-1} and 1180 and 1250 cm^{-1} associated with the antisymmetric and symmetric bend of the hydronium ion, respectively.[43] Figure 5 also shows that HCl is produced as a volatile species during electron beam irradiation of the CCl_4/H_2O(ice) films. These results suggest that HCl undergoes competitive electron-stimulated desorption ($HCl_{(ads)} + e^- \rightarrow HCl_{(g)}$), as well as ionization ($HCl_{(ads)} \rightarrow H_3O^+_{(ads)} + Cl^-_{(ads)}$), within the ice film.

Trichloromethyl Radical ($^\bullet CCl_3$). Phosgene is postulated to result from the reaction between the trichloromethyl radical and either hydroxyl radicals or molecular oxygen[19,57,31,8] (Scheme 1). In the case of hydroxyl radicals, the reaction proceeds thus

$$^\bullet CCl_3 + {}^\bullet OH \rightarrow HOCCl_3 \quad (9)$$

$$HOCCl_3 \rightarrow HCl + COCl_2 \quad (10)$$

The $HOCCl_3$ intermediate is postulated to undergo rapid unimolecular decomposition, leading to the production of phosgene and HCl. Furthermore, because phosgene does not originate from any reaction associated with the dichlorocarbene, the observation of phosgene in the present investigation is taken as evidence for the involvement and formation of the $^\bullet CCl_3$ species during electron beam irradiation.

Reaction between molecular oxygen and the trichloromethyl radical leads to the formation and subsequent decomposition of the peroxyl radical:[49]

$$^\bullet CCl_3 + O_2 \rightarrow CCl_3OO^\bullet \qquad (k = 3.3 \times 10^9\ M^{-1}\ s^{-1}) \quad (4)$$

Subsequent decay of the peroxyl radical is suggested to proceed via oxygen elimination as a result of peroxyl radical−radical reactions:

$$2CCl_3OO^\bullet \rightarrow O_2 + 2CCl_3O^\bullet \quad (11)$$

$$CCl_3O^\bullet \rightarrow CCl_2O + Cl^\bullet \quad (12)$$

Reactions involving the $Cl^\bullet$ radical are postulated to result in H_3O^+ and Cl^- production through reactions such as:

$$Cl^\bullet + H_2O \rightarrow HCl + {}^\bullet OH \quad (13)$$

$$H_2O + HCl \rightarrow H_3O^+ + Cl^- \quad (8)$$

Chlorine radicals can also form molecular chlorine as a result of bimolecular coupling:

$$Cl^\bullet + Cl^\bullet \rightarrow Cl_2 \quad (14)$$

The absence of any mass spectral intensity at $m/q = 70$, 72, or 74 (Figure 4), however, suggests that bimolecular chlorine radical coupling reactions in the ice film leading to the production of volatile Cl_2 ($Cl^\bullet + Cl^\bullet \rightarrow Cl_2$) is not a significant component of the overall reaction scheme. In principle, Cl_2 produced in the ice film could also undergo hydrolysis:

$$Cl_2 + H_2O \rightarrow HOCl + HCl \qquad (k = 30.5\ s^{-1} \quad \text{at} \quad 30\ ^\circ C)^{58} \quad (15)$$

On the basis of the relatively slow rate of reaction anticipated under our experimental conditions ($\sim 1 \times 10^{-21}$ s^{-1} at 100 K),[58] however, coupled with the volatility of Cl_2, we anticipate that any Cl_2 formed would escape into the gas phase rather than undergo hydrolysis.

In contrast with the carbon−carbon coupling of the $:CCl_2$ intermediate, however, no IR active bands associated with $^{12}C_2Cl_6$ ($\delta(CCl_3) = 778$ cm^{-1}) were observed.[51] On the basis of the physical properties of C_2Cl_4 and C_2Cl_6 ($\Delta H_{vap}(C_2Cl_4) = 35$ kJ mol^{-1}; $\Delta H_{vap}(C_2Cl_6) = 46$ kJ mol^{-1}),[56] both C_2 species should be thermally stable in the film at 100 K. Consequently, it appears that carbon−carbon coupling involving the $^\bullet CCl_3$ intermediate is only a minor reaction channel:

$$^\bullet CCl_3 + {}^\bullet CCl_3 \rightarrow C_2Cl_6 \quad (16)$$

The importance of $:CCl_2$ rather that $^\bullet CCl_3$ coupling during electron beam irradiation of CCl_4/H_2O (ice) films is also consistent with low-temperature (12 K) matrix IR studies on low-energy impact on CCl_4 in which $:CCl_2$, $^\bullet CCl_3$, and C_2Cl_4 were identified but C_2Cl_6 was not observed.[23]

On the basis of the observed stability of CH_2Cl_2 ($\Delta H_{vap}(CH_2Cl_2) = 28-29$ kJ mol^{-1}) in the water (ice) film at 100 K,[54] $CHCl_3$ ($\Delta H_{vap}(CHCl_3) = 29-31$ kJ mol^{-1}) produced during electron beam irradiation of CCl_4/H_2O(ice) films is also expected to remain trapped at ~100 K. Consequently, the absence of any IR modes associated with $CHCl_3$ (e.g., $\delta(CH) \approx 1219$ cm^{-1})[51]

in Figure 2 suggests that reactions between hydrogen radicals, generated from the electron beam irradiation of ice, and trichloromethyl radicals do not represent a dominant reaction pathway in the overall reaction scheme:

$$^{\bullet}CCl_3 + {}^{\bullet}H \rightarrow CHCl_3 \quad (17)$$

It should also be noted that the lack of any hydrolysis reactions associated with $^{\bullet}CCl_3$ in Scheme 1 is consistent with the results of previous studies.[50]

Electron-Stimulated Decomposition of Phosgene. The instability of phosgene in the ice film under the influence of electron beam irradiation is evidenced by the time-dependent evolution of the $^{13}COCl_2$ $\upsilon(^{13}C{=}O)$ mode at 1758 cm^{-1} shown in Figure 4. In the present study, we propose that carbon dioxide and carbon monoxide are both produced by the electron-stimulated decomposition of phosgene:

$$COCl_2 + e^-_{(aq)} \rightarrow {}^{\bullet}COCl + Cl^- \quad (18)$$

$^{\bullet}COCl$ can then react with molecular oxygen to produce CO_2 in a mechanism analagous to the decomposition of $CCl_3OO^{\bullet}$; thus,

$$^{\bullet}COCl + O_2 \rightarrow {}^{\bullet}OOCOCl \quad (19)$$

$$2{}^{\bullet}OOCOCl \rightarrow 2{}^{\bullet}OCOCl + O_2 \quad (20)$$

$$^{\bullet}OCOCl \rightarrow CO_2 + Cl^{\bullet} \quad (21)$$

or with hydroxyl radicals,

$$^{\bullet}COCl + {}^{\bullet}OH \rightarrow (HO)COCl \quad (22)$$

$$(HO)COCl \rightarrow CO_2 + HCl \quad (23)$$

Alternatively, $^{\bullet}COCl$ can undergo unimolecular decomposition to yield CO and $Cl^{\bullet}$:

$$^{\bullet}COCl \rightarrow CO + Cl^{\bullet} \quad (24)$$

A similar set of reaction steps involving the electron-stimulated decomposition of phosgene has been proposed in experimental[59] and theoretical[60] studies of carbon tetrachloride decomposition by electron beam atmospheric plasmas in dry air. On the basis of the proposed reaction scheme, the phosgene concentration in the ice film is determined by the following general reaction scheme involving the $^{\bullet}CCl_3$ intermediate:

$$CCl_4 + e^-_{(aq)} \rightarrow {}^{\bullet}CCl_3 \rightarrow COCl_2 + e^-_{(aq)} \rightarrow CO/CO_2 \quad (25)$$

At short irradiation times, the phosgene concentration increases due to the abundance of CCl_4 in the ice film, while for longer exposures the $COCl_2$ concentration is depleted by electron-stimulated decomposition (Figure 4).

CO_2 Formation. As stated above, CO_2 formation can arise from the electron-stimulated decomposition of phosgene. CO_2 can also result from the reaction between CO and hydroxyl radicals before CO escapes from the film:

$$CO + {}^{\bullet}OH \rightarrow CO_2 + H \quad (26)$$

Separate experiments revealed that in the absence of electron beam irradiation the $^{13}CO_2$ concentration in ice films was constant over a time period of several hours, as measured by the IR band intensity at 2272 cm^{-1} ($\upsilon_s(^{13}C{=}O)$). This result indicates that $^{13}CO_2$ is lost from the film as a result of electron-stimulated desorption.

In water, carbon dioxide production from phosgene is normally ascribed to hydrolysis, which under ambient conditions is rapid ($k = 70\ s^{-1}$ at 50 °C):[61,62]

$$COCl_2 + H_2O \rightarrow CO_2 + 2HCl \quad (27)$$

Separate experiments, however, revealed that in the absence of electron beam irradiation the $^{13}COCl_2$ concentration in ice films was constant over a time period of several hours, as measured by the IR band intensity at 1758 cm^{-1} ($\upsilon(^{13}C{=}O)$). This indicates that, under the low-temperature (~100 K) conditions employed in the present study, the degradation of phosgene is not a result of hydrolysis. Carbon dioxide production also could, in principle, originate from the reaction of formate, produced as the result of CO base hydrolysis, with hydroxyl radicals:[22]

$$CO + OH^- \rightarrow HCOO^- \quad (28)$$

$$HCOO^- + {}^{\bullet}OH \rightarrow\rightarrow CO_2 \quad (29)$$

The absence of IR bands associated with formate during electron beam irradiation, however, coupled with the likely acidic nature of the solution (resulting from HCl production), leads us to conclude that base hydrolysis is not a route for CO_2 production in the present study.

Under low-temperature (~100 K) conditions, it is apparent from the reaction mechanism proposed (Scheme 1) and the preceding discussion that reactivity is governed by radical−neutral or radical−radical interactions. In contrast, under ambient conditions, reactions between neutral species (e.g., $COCl_2 + H_2O \rightarrow CO_2 + 2HCl$, $Cl_2 + H_2O \rightarrow HCl + HOCl$, or both) are far more important.[8,58] The origin of this difference lies in the fact that reactions involving radical species are typically characterized by negligible activation barriers and thus have a much weaker temperature dependence compared to reactions involving neutral molecules. Another consequence of the low temperatures employed in the present study is that the mobility of reactive species will be significantly reduced compared to electron beam irradiation experiments carried out at room temperature. As a result, reactions are expected to occur principally as a result of encounters between species in close proximity to one another within the ice film.

Electron-Stimulated Desorption Processes in CCl_4/H_2O-(Ice) Films. The mass spectral information contained in Figure 5 can be used to provide information on the nature and relative importance of various electron-stimulated processes occurring in the CCl_4/H_2O(ice) films**.** Thus, the appearance of intensity at $m/q = 18$, 17, and 16 in Figure 5c and d shows that electron beam irradiation results in electron-stimulated desorption of H_2O. In contrast, no mass spectral features associated with molecular $^{12/13}CCl_4$, for example, the $^{12}C^{35/37}Cl$ doublet feature at $m/q = 47/49$, were observed during electron beam irradiation of $^{12}CCl_4/H_2O$(ice) films (Figure 5c). This indicates that, under the experimental conditions employed in the present investigation, electron-stimulated desorption of CCl_4 is negligible compared to the rate of electron-stimulated C−Cl bond cleavage. Interestingly, no electron-stimulated desorption of phosgene is observed, evidenced by the lack of mass spectral intensity at $m/q = 63$, corresponding to the largest cracking fragment of $^{12}COCl_2$. This suggests that, in general, electron-stimulated C−Cl bond cleavage dominates over desorption for C−Cl-containing species. In fact, on the basis of RAIRS and mass spectrometry results it appears that chlorine is partitioned mainly

as HCl. It should be noted, however, that a number of charged and/or reactive species are also expected to be ejected into vacuum during the electron beam irradiation of CCl_4/H_2O(ice) films, including Cl^-, $^\bullet OH$, and H^-.[25,32,33] These species cannot be detected using our experimental arrangement, although reactions of Cl^- and $Cl^\bullet$ with the chamber walls may contribute to the overall HCl signal observed (Figure 5).

One- vs Two-Electron Transfer to CCl_4. The initial dissociative electron attachment to CCl_4 can occur through an overall one- or two-electron-transfer process, leading to the formation of the trichloromethyl radical ($^\bullet CCl_3$) or dichlorocarbene ($:CCl_2$) intermediates, respectively.[18] In the present investigation, C_2Cl_4 is observed as a reaction product in the absence of any detectable C_2Cl_6. Furthermore, even in more dilute CCl_4/H_2O(ice) films than those used in the present study, CO (generated from reaction 6) rather than CO_2 was found to be the predominant carbon-containing gas-phase desorption product. On the basis of the similar quadrupole sensitivities toward CO (1.0) and CO_2 (0.7), the mass spectral information contained in Figure 5 suggests that reactions associated with dichlorocarbene represent the dominant reaction pathways, implicating the two-electron transfer leading to the production of the dichlorocarbene ($:CCl_2$) as the main path for CCl_4 degradation in the CCl_4/H_2O(ice) system (Scheme 1). This assertion is also supported by the fact that two-electron transfer to CCl_4 is thermodynamically more favorable than one-electron transfer.[18]

Role of Molecular Oxygen. The role of molecular oxygen, generated *in situ* by electron beam irradiation of CCl_4/H_2O-(ice) films, is clearly implicated by the results of this investigation. The efficient production of molecular oxygen during low energy (<100 eV) electron irradiation of water was initially reported by Orlando and co-workers[31] who noted an electron energy threshold of ~10 eV, corresponding to the valence band excitation of ice. The mechanism of molecular oxygen production was proposed to occur through a HO_2 or H_2O_2 precursor rather than O atom recombination. Further electronic excitation leads to the dissociation of the precursor and the formation of O_2.

Irrespective of the detailed mechanism responsible for O_2 production, it is clear that molecular oxygen, generated *in situ* by electron beam irradiation, plays a role in determining the mechanism of CCl_4 degradation in ice films. This is evidenced by the decrease in the O_2 signal during electron beam irradiation of CCl_4/H_2O(ice) films studied despite the continued production of significant amounts of H_2 (compare Figure 5 spectrum b with spectra c and d). This effect is ascribed to the efficient consumption of O_2 generated by electron beam irradiation in the film as a result of reactions with the trichloromethyl radical:

$$^\bullet CCl_3 + O_2 \rightarrow CCl_3OO^\bullet \qquad (k = 3.3 \times 10^9\ M^{-1}\ s^{-1}) \quad (4)$$

In the context of chlorocarbon remediation, oxygen is often required to ensure efficient degradation. Results from this study, therefore, indicate that, in addition to its capacity for C−Cl bond cleavage, ionizing radiation (e.g., VUV, gamma radiation) may be used as a means to generate molecular oxygen *in situ*. This could be important in ground water or vadose zone remediation situations where it is difficult to supply oxygen into the reaction medium directly. In addition to these potential practical implications, results from this investigation indicate that molecular oxygen must also be considered in models describing electron-beam- and plasma-based remediation of chlorocarbons in oxygen-deficient aqueous environments.

Conclusions

Electron-stimulated reactions of carbon tetrachloride in ice films produce trichloromethyl ($^\bullet CCl_3$) and dichlorocarbene ($:CCl_2$) intermediates. Dichlorocarbene reacts further to produce either tetrachloroethylene (C_2Cl_4) through a carbon−carbon coupling reaction or carbon monoxide and hydrochloric acid as a result of hydrolysis. In contrast, reactions involving the trichloromethyl radical lead to the production of phosgene ($COCl_2$). Subsequent electron-stimulated decomposition of phosgene produces CO and CO_2, as well as hydrochloric acid. In the presence of CCl_4, the electron-stimulated production of molecular oxygen, detected as a gas-phase product in the electron beam irradiation of ice, is efficiently quenched. The observation of C_2Cl_4 and the dominance of CO over CO_2 as a volatile desorption product is consistent with the idea that a two-electron-transfer process dominates CCl_4 degradation. In the context of chlorocarbon remediation, the role of ionizing radiation in generating molecular oxygen *in situ* from water in otherwise oxygen-deficient environments has also been identified.

Acknowledgment. Support for this research was provided by the National Science Foundation (Grant No. CHE-0089168) as part of the Collaborative Research Activities in Environmental Molecular Science in Environmental Redox-Mediated Dehalogenation Chemistry at the Johns Hopkins University. The authors would also like to acknowledge the help of Brett Showalter in calculating the isotopic shifts anticipated for $^{12}C/^{13}C$ tetrachloroethylene and phosgene.

References and Notes

(1) Gerhartz, W. *Ulmann's Encyclopedia of Industrial Chemistry*; VCH Verlagsgesallschaft: Weinheim, Germany, 1986.
(2) Norstrom, R. J.; Simon, M.; Muir, D. C. G.; Schweinsburg, R. E. *Environ. Sci. Technol.* **1988**, *22*, 1063.
(3) Jeffers, P. M.; Ward, L. M.; Woytowitch, L. M.; Wolfe, N. L. *Environ. Sci. Technol.* **1989**, *23*, 965.
(4) Haag, W. R.; Yao, C. C. D. *Environ. Sci. Technol.* **1992**, *26*, 1005.
(5) Mabey, W.; Mill, T. *J. Phys. Chem. Ref. Data* **1978**, *7*, 383.
(6) Taylor, P. H.; Dellinger, B.; Tirey, D. A. *Int. J. Chem. Kinet.* **1991**, *23*, 1051.
(7) Sabin, F.; Tuerk, T.; Vogler, A. *J. Photochem. Photobiol.* **1992**, *63*, 99.
(8) Hua, I.; Hoffmann, M. R. *Environ. Sci. Technol.* **1996**, *30*, 864.
(9) Criddle, C. S.; McCarthy, P. L. *Environ. Sci. Technol.* **1991**, *25*, 973.
(10) Galli, R.; McCarty, P. L. *Appl. Environ. Microbiol.* **1989**, *55*, 837.
(11) Koper, O.; Lagadic, I.; Klabunde, K. J. *Chem. Mater.* **1997**, *9*, 838.
(12) Roberts, A. L.; Totten, L. A.; Arnold, W. A.; Burris, D. R.; Campbell, T. J. *Environ. Sci. Technol.* **1996**, *30*, 2654.
(13) Kriegman-King, M. R.; Reinhard, M. *Environ. Sci. Technol.* **1994**, *28*, 692.
(14) Tobien, T.; Cooper, W. J.; Nickelsen, M. G.; Pernas, E.; O'Shea, K. E.; Asmus, K.-D. *Environ. Sci. Technol.* **2000**, *34*, 1286.
(15) Cooper, W. J.; Cadavid, E.; Nickelsen, M. G.; Lin, K.; Kurucz, C. N.; Waite, T. D. *J. Am. Water Works Assoc.* **1993**, *85* (Sept), 106.
(16) Mak, F. T.; Zele, S. R.; Cooper, W. J.; Kurucz, C. N.; Waite, T. D.; Nickelsen, M. G. *Water Res.* **1997**, *31*, 219.
(17) Balkas, T. I. *Int. J. Radiat. Phys. Chem.* **1972**, *4*, 199.
(18) Choi, W.; Hoffmann, M. R. *J. Phys. Chem.* **1996**, *100*, 2161.
(19) Monig, J.; Bahnemann, D.; Asmus, K.-D. *Chem.-Biol. Interact.* **1983**, *47*, 15.
(20) Choi, W.; Hoffmann, M. R. *Environ. Sci. Technol.* **1995**, *29*, 1646.
(21) Hooker, P. D.; Klabunde, K. J. *Environ. Sci. Technol.* **1994**, *28*, 1243.
(22) Robinson, E. A. *J. Chem. Soc.* **1961**, 1663.
(23) Suzer, S.; Andrews, L. *Chem. Phys. Lett.* **1988**, *150*, 13.
(24) Lu, Q.-B.; Madey, T. E. *J. Phys. Chem. B* **2001**, *105*, 2779.
(25) Lu, Q.-B.; Madey, T. E. *Surf. Sci.* **2000**, *451*, 238.
(26) Lu, Q.-B.; Madey, T. E. *J. Chem. Phys.* **1999**, *111*, 2861.
(27) Kimmel, G. A.; Orlando, T. M.; Vezina, C.; Sanche, L. *J. Chem. Phys.* **1994**, *101*, 3282.

(28) Kimmel, G. A.; Tonkyn, R. G.; Orlando, T. M. *Nucl. Instrum. Methods Phys. Res., Sect. B* **1995**, *101*, 179.

(29) Kimmel, G. A.; Orlando, T. M.; Cloutier, P.; Sanche, L. *J. Phys. Chem.* **1997**, *101*, 6301.

(30) Orlando, T. M.; Kimmel, G. A.; Simpson, W. C. *Nucl. Instrum. & Methods in Phys. Res. B* **1999**, *157*, 183.

(31) Sieger, M. T.; Simpson, W. C.; Orlando, T. M. *Nature* **1998**, *394*, 554.

(32) Simpson, W. C.; Parenteau, L.; Smith, R. S.; Sanche, L.; Orlando, T. M. *Surf. Sci.* **1997**, *390*, 86.

(33) Prince, R. H.; Sears, G. N.; Morgan, F. J. *J. Chem. Phys.* **1976**, *64*, 3978.

(34) Noell, J. O.; Melius, C. F.; Stulen, R. H. *Surf. Sci.* **1985**, *115*, 119.

(35) Rowntree, P.; Parenteau, L.; Sanche, L. *J. Chem. Phys.* **1991**, *94*, 8570.

(36) Carlo, S. R.; Torres, J.; Fairbrother, D. H. *J. Phys. Chem. B* **2001**, *105*, 6148.

(37) *The Handbook of X-ray Photoelectron Spectroscopy*; Perkin-Elmer Corporation: 1979.

(38) Koper, O. B.; Wovchko, E. A.; Glass, J. A., Jr.; Yates, J. T., Jr.; Klabunde, K. J. *Langmuir* **1995**, *11*, 2054.

(39) Abramovitz, S.; Comeford, J. *J. Spectrochim. Acta* **1964**, *21*, 1479.

(40) Ballinger, T. H.; Yates, J. T., Jr. *J. Phys. Chem.* **1992**, *96*, 1417.

(41) Hannus, I.; Kiricsi, I.; Tasi, G.; Fejes, P. *Appl. Catal.* **1990**, *66*, L7.

(42) Driessen, M. D.; Goodman, A. L.; Miller, T. M.; Zaharias, G. A.; Grassian, V. H. *J. Phys. Chem. B* **1998**, *102*, 549.

(43) Delzeit, L.; Rowland, B.; Devlin, J. P. *J. Phys. Chem.* **1993**, *97*, 10312.

(44) Carlo, S. R.; Grassian, V. H. *J. Phys. Chem. B* **2000**, *104*, 86.

(45) Barone, S. B.; Zondlo, M. A.; Tolbert, M. A. *J. Phys. Chem. B* **1999**, *103*, 9717.

(46) Blanchard, J. L.; Roberts, J. T. *Langmuir* **1994**, *10*, 3303.

(47) Parrett, J. W.; Sumner, J. P.; Devore, T. C. *Environ. Sci. Technol.* **1999**, *33*, 1691.

(48) Calza, P.; Minero, C.; Pelizzetti, E. *Environ. Sci. Technol.* **1997**, *31*, 2198.

(49) Asmus, K.-D.; Bahnemann, D.; Krischer, K.; Lal, M.; Monig, J. *Life Chem. Rep.* **1985**, *3*, 1.

(50) Yu, Y.; Wang, S.; Liu, X.; Hou, J.; Hou, H.; Yao, S.; Wang, W. *Spectrosc. Lett.* **1999**, *32*, 983.

(51) Shimanouchi, T. *Tables of Molecular Vibrational Frequencies*; National Bureau of Standards: Washington, DC, 1972; Consolidated Volume I, p 1.

(52) Frisch, M. J.; Trucks, G. W.; Schlegel, H. B.; Scuseria, G. E.; Robb, M. A.; Cheeseman, J. R.; Zakrzewski, V. G.; Montgomery, J. A., Jr.; Stratmann, R. E.; Burant, J. C.; Dapprich, S.; Millam, J. M.; Daniels, A. D.; Kudin, K. N.; Strain, M. C.; Farkas, O.; Tomasi, J.; Barone, V.; Cossi, M.; Cammi, R.; Mennucci, B.; Pomelli, C.; Adamo, C.; Clifford, S.; Ochterski, J.; Petersson, G. A.; Ayala, P. Y.; Cui, Q.; Morokuma, K.; Malick, D. K.; Rabuck, A. D.; Raghavachari, K.; Foresman, J. B.; Cioslowski, J.; Ortiz, J. V.; Stefanov, B. B.; Liu, G.; Liashenko, A.; Piskorz, P.; Komaromi, I.; Gomperts, R.; Martin, R. L.; Fox, D. J.; Keith, T.; Al-Laham, M. A.; Peng, C. Y.; Nanayakkara, A.; Gonzalez, C.; Challacombe, M.; Gill, P. M. W.; Johnson, B. G.; Chen, W.; Wong, M. W.; Andres, J. L.; Head-Gordon, M.; Replogle, E. S.; Pople, J. A. *Gaussian 98*, revision A.7; Gaussian, Inc.: Pittsburgh, PA, 1998.

(53) Weckhuysen, B. M.; Mestl, G.; Rosynek, M. P.; Krawietz, T. R.; Haw, J. F.; Lunsford, J. H. *J. Phys. Chem. B* **1998**, *102*, 3773.

(54) Wagner, A. J.; Wolfe, G.; Vecitis, C.; Fairbrother, D. H. Unpublished work.

(55) Pliego, J. R.; DeAlmeida, W. B. *J. Phys. Chem.* **1996**, *100*, 12410.

(56) *CRC Handbook of Chemistry and Physics*, 69th ed.; CRC Press: Boca Raton, FL, 1988−89.

(57) Choi, W.; Hoffmann, M. R. *Environ. Sci. Technol.* **1997**, *31*, 89.

(58) Wang, T.; Margerum, D. *Inorg. Chem.* **1994**, *33*, 1050.

(59) Koch, M.; Cohn, D. R.; Patrick, R. M.; Schuetze, M. P.; Bromberg, L.; Reilly, D.; Hadidi, K.; Thomas, P.; Falkos, P. *Environ. Sci. Technol.* **1995**, *29*, 2946.

(60) Nichipor, H.; Dashouk, E.; Chmielewski, A. G.; Zimek, Z.; Bulka, S. *Radiat. Phys. Chem.* **2000**, *57*, 519.

(61) Manogue, W. H.; Pigford, R. L. *Am. Inst. Chem. Eng. J.* **1960**, *6*, 494.

(62) Mertens, R.; vonSonntag, C.; Lind, J.; Merenyi, G. *Angew. Chem., Int. Ed. Engl.* **1994**, *33*, 1259.